STIS Next Generation Spectral Library
(Version 1, March 2008)

Don Lindler, Sigma Space Corporation, Don.J.Lindler@nasa.gov
Sara R Heap, NASA/Goddard Space Flight Center, Sara.R.Heap@nasa.gov

The STIS Next Generation Spectral Library contains STIS spectra of 370 stars observed in HST programs 9088, 9786, and 10222. Each spectrum includes spectral segments from gratings G230LB, G430L, and G750L merged to form a single spectrum covering ~0.2-1.0 μ. NGSL spectra were constructed via custom pipeline processing (section 2) followed by corrections for in-order scatter by grating G230LB (section 3.1) and corrections for throughput variations caused by the mis-centering of the target in the 0.2 arcsecond-wide slit. (section 3.2). A summary of the observations and derived stellar parameters is given in section 4.

1. File Content and Format

Each data file is a FITS binary table. The primary FITS header contains the following information:

FITS File primary header

```
SIMPLE  =                    T /image conforms to FITS standard
BITPIX  =                   16 /bits per data value
NAXIS   =                    0 /number of axes
EXTEND  =                    T /file may contain extensions
TARGNAME= 'BD+112998'          /target name
SPECTYPE= 'composite'          /Spectra type
TELESCOP= 'HST     '           /observatory
INSTRUME= 'STIS    '           /instrument
FILENAME= 'h_stis_ngsl_bd+112998_v1.fits' /
RA      =        3713.54743480 /Right Ascension (deg)
DEC     =        10.9976309090 /Declination (deg)
EQUINOX =              2000.00 /equinox of celestial coord. system
APERTURE= '52X0.2          '   /
GRATING = 'G230LB, G430L, G750L' /
OBSDATE = '2004-04-10'         /date of observation YYYY-MM-DD
EXPSTART=        53105.9428153 /Start time of obs. sequence (MJD)
EXPEND  =        53105.9637181 /End time of obs. sequence (MJD)
MINWAVE =        1675.66137068 /Minimum wavelength
MAXWAVE =        10198.7137562 /Maximum wavelength
MAXFLUX =          9.14272E-13 /Maximum Flux in erg/sec/cm^2/Angstrom
OFFSETPX=            -0.324710 /Offset of star from center of slit
                                                            (pixels)
```

```
DATAQUAL= 'good    '           /Data Quality: good or suspect
HIPP    =                80822 /Hipparcos number
FITQUAL =                    1 /Fit Quality: 1=good, 2=poor, 3=not
fit
FIT_RMS =            0.0220523 /RMS of FIT
TEFF    =              5875.56 /Effective Temperature (K)
LOG_G   =              2.77228 /Log Surface Gravity
LOG_Z   =            -0.600000 /Log Abundance (with respect to Solar)
ALPHA   = 'n       '           /"a" if alpha-enhanced
EBMV    =             0.125778 / E(B-V) derived from fit
DPC     =              606.252 /Distance (Parsecs)
HISTORY STIS Next Generation Spectral Library, Version 1, 27-Feb-2008
HISTORY  --------------------------------------------
HISTORY        FILENAME        OPT_ELEM   TEXPTIME
HISTORY  --------------------------------------------
HISTORY  o8ru1p010_raw.fits   G230LB         600.000
HISTORY  o8ru1p020_raw.fits   G230LB         600.000
HISTORY  o8ru1pjiq_raw.fits   G430L          30.0000
HISTORY  o8ru1pjjq_raw.fits   G430L          30.0000
HISTORY  o8ru1pjkq_raw.fits   G750L          30.0000
HISTORY  o8ru1pjlq_raw.fits   G750L          30.0000
END
```

OFFSETPX gives the offset of the target in pixels (0.05 arcsecond/pixel) from the center of the slit as measured using the G750L fringe flats (Section 3.2). **DATAQUAL** is used to flag data that may be suspect because of a large centering error within the slit. The data are flagged as suspect if the offset error is more than 0.9 pixels. As center of the target star moves off the slit, the estimated offset computed from the fringe flat does not continue to increase and may even get smaller because the fringe flat is being correlated with the wings of the stellar PSF. To identify this problem, we also flag data as suspect if the star's visual magnitude determined from the observed spectrum differs by more than 0.1 from the visual magnitude given in the Tycho II catalog or if the B-V magnitude differs by more than 0.3.

FITQUAL gives an indicator of the quality of the fit of the stellar model to the spectrum:

1 – indicates that a good fit was found.
2 – indicates that we were able to fit the spectrum but the RMS (see section 4) was greater 0.035
3 – indicates that no fit was possible or the RMS was greater than 0.08

If a fit was performed, keywords **FIT_RMS, TEFF, LOG_G, LOG_L, ALPHA, EBMV,** and **DPC** will be populated. **DPC** is the estimated distance in parsecs based on the best fit model that falls on a Victoria-Regina isochrone with the restriction that the parallax for the distance falls within a 2-sigma error of new Hipparcos catalog parallax.

The file's binary table extension contains five columns:

WAVELENGTH – wavelength in Angstroms

FLUX – observed flux in ergs/cm^2/second/Angstrom
STATERR – propagated counting statistical errors.
FLUX_UNRED – flux after extinction correction using the E(B-V) computed during model fitting (section 4)
FLUX_10PC – Flux scaled to a stellar distance of 10 parsecs (absolute flux). The distance was computed during the model fitting (section 4) allowing up to a two-sigma error in the parallax from the Hipparcos catalog.

2. Improvements to the Standard Pipeline Calibration

The following improvements to the standard STIS pipeline processing were used to process the individual NGSL observations:

1) New spectral trace files were produced used. These were constructed from the average spectral y-position versus x-position for the 52X0.2E1 aperture for all of the NGSL stars.
2) Custom fringe flats were constructed for each of the G750L observations using the tungsten lamp observation associated with the visit.
3) A more appropriate background subtraction was used. The standard pipeline uses only a lower background taken 300 pixels below the spectrum for the E1 aperture position. We used both an upper and lower background taken much closer to the spectrum (30 pixels).
4) A larger extraction slit height (11 instead of 7) was used to improve overall photometric precision at the cost of some loss in S/N.
5) Custom wavelength dispersion coefficients were created for the E1 aperture position.
6) Wavecals were not taken with the stellar observations. Zero point offsets were computed for each spectrum using the positions and wavelengths of strong stellar features.
7) Custom sensitivity curves applicable to our background subtraction method were created for the 52X0.2E1 aperture using observations of BD+75D325 centered in the aperture.

3. Post Pipeline Processing.

After routine pipeline processing the following steps were used to construct the final composite spectra:

1. The observations for each grating were obtained at two slightly different y-positions along the slit. These were co-added after rejection of cosmic rays and hot pixels.
2. The observations of the three gratings were merged with an average taken in the overlap region (2990 – 3060 Angstroms for G230LB and G430L, 5500-5650 Angstroms for G430L and G750L).
3. In-order grating scatter was subtracted for G230LB (Section 3.1).

4. A correction was performed for the slit throughput for targets not centered in the slit (Section 3.2)

3.1 G230LB Scattered Light Correction

There is significant in-order grating scatter which affects the flux values for G230LB. This scattered light is particularly evident for very cool stars. We have modeled this scatter by:

$$SC = C0(1+Slope*x)$$

Where SC is the scattered light in counts/second/pixel in the extracted net spectrum, X is the pixel number from 0 to 1023, C0 is the amount of scattered light, and Slope is the slope of the scattered light profile across the detector.

To construct the model, we selected 103 red stars in the NGSL library with a B-V>1.1, Vmag<10, and the position of the target within 0.9 pixels of the center of the 52X0.2E1 aperture. (as measured using the G750L fringe flat, see section 3.2).

For each star, the scattered light was fit by a straight line between pixels 10 and 220 where actual stellar flux should be negligible for the 103 red stars.

$$\text{Scattered light} = c0 + c1*x \qquad (1)$$

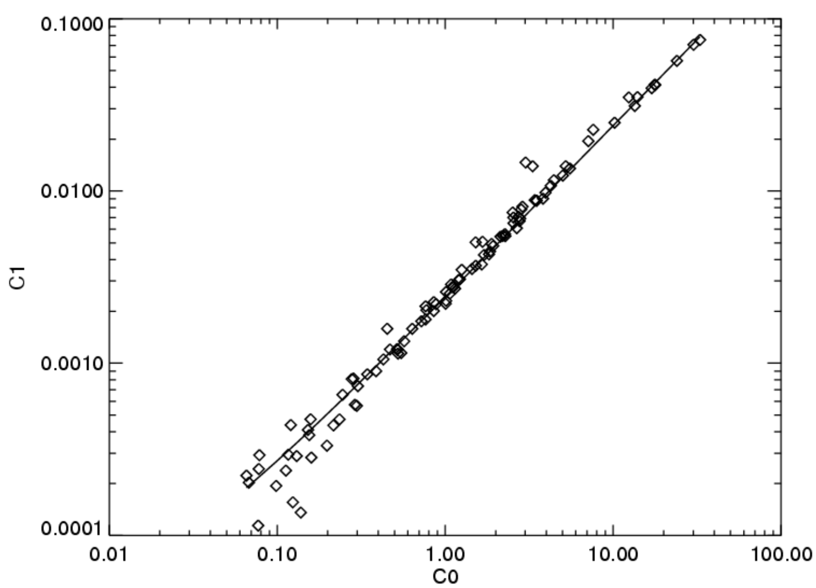

Figure 1 (G230LB Slope of the scattered light)

Figure 1 shows the values of c1 plotted versus c0.This was fit by a straight line with a slope of 0.0024.

Thus equation 1 can be written as:

$$\text{Scattered Light} = c0\ (1+0.0024*x) \qquad (2)$$

We model the amount of scatter, c0, by:

$$c0 = A\int C(\lambda)/\lambda^{n}$$

Where $C(\lambda)$ is the scattered light in counts/second and n is a selectable exponent. The integration is done from 2000 to 10,000 Angstroms. The limits of integration present a problem since we only get the net count rates below 3060 Angstroms for a G230LB observation. To get the net count rates for G230LB beyond the portion visible on the detector we use the flux measured by the G430L and G750L gratings. These can be converted to G230LB count rates using the combined G230L component efficiencies measured prior to launch. Figure 2 shows the G230L sensitivity determined from the combined component efficiencies (solid line) compared to the post-launch G230LB sensitivity shown as a dashed line.

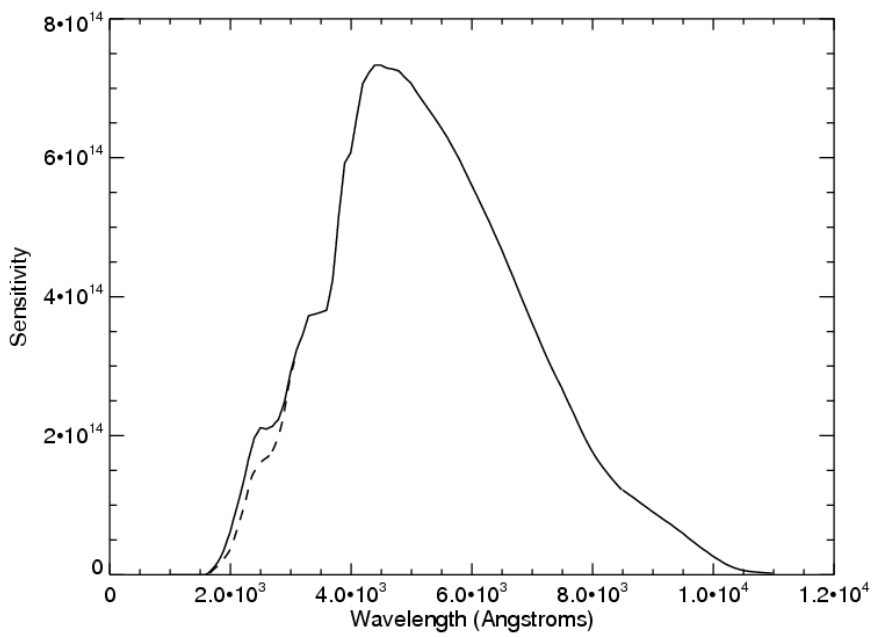

Figure 2 (G230LB Sensitivity)

We have chosen the exponent, n=3, to minimize the scatter in the fit for the 103 NGSL red stars. Figure 3 shows a plot of C0 versus the integral of the count rate divided by wavelength cubed. The slope of the fitted line gives a value of A=5523.

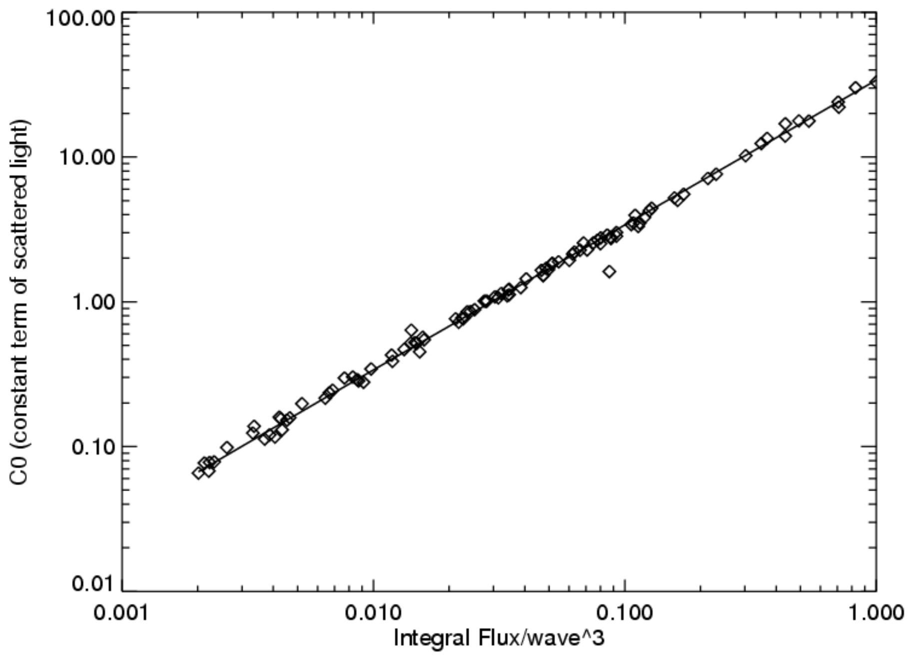

Figure 3 (G230LB scattered light)

Thus the final scattered light correction algorithm is given by:

1. Process the observations for all three gratings using no scattered light correction.
2. Merge the flux from the three gratings and divide by the G230LB sensitivity from 2000 to 10000 Angstroms to get G230LB count rates.
3. Integrate the count rate divided by the wavelength cubed from 2000 to 10000 Angstroms and multiply by 5523 to get C0.
4. Subtract C0*(1+0.0024)*X from the G230L net spectrum and multiply by the post-launch sensitivity curve.

One concern is that the straight line fit to the scattered light which is very good for the first 220 pixels may not an accurate extrapolation to pixel 1023. To test the extrapolation we can use the overlap region between the G230LB and G430L gratings. Figure 4 shows the ratio of the G430L/G230LB measured flux from 2980 to 3040 Angstroms versus B-V when no G230LB scattered light correction is performed. Stars with a B-V greater than 1 show the ratio becoming smaller as B-V increases indicating that the G230LB flux values are too large. The same plot (Figure 5) when the scattered light correction is done shows much better results for these redder stars.

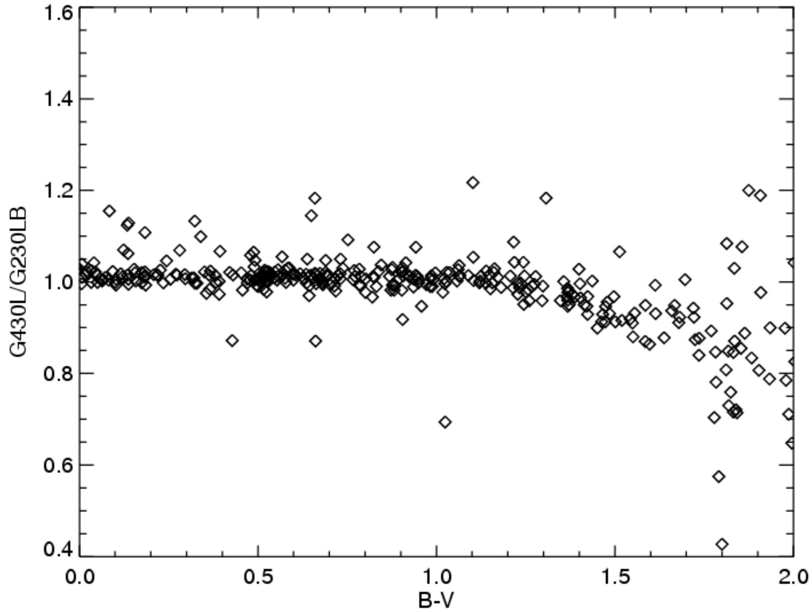

Figure 4 (No G230LB scattered light correction)

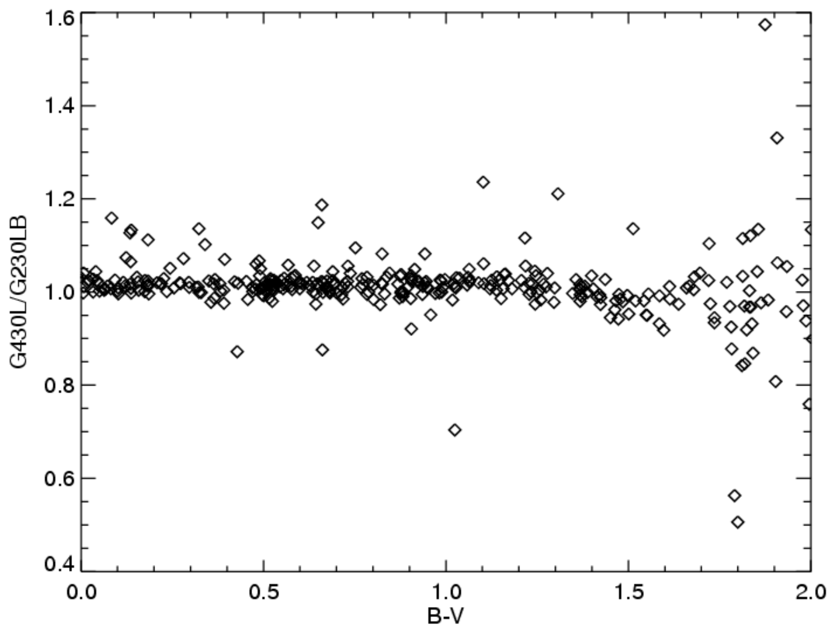

Figure 5 (With G230LB Scattered light correction)

Figure 6 shows an example of the G230LB spectrum before (black) and after (green) scattered light correction. For comparison, the red plot shows a STIS Echelle observation (E230M) binned to the same resolution.

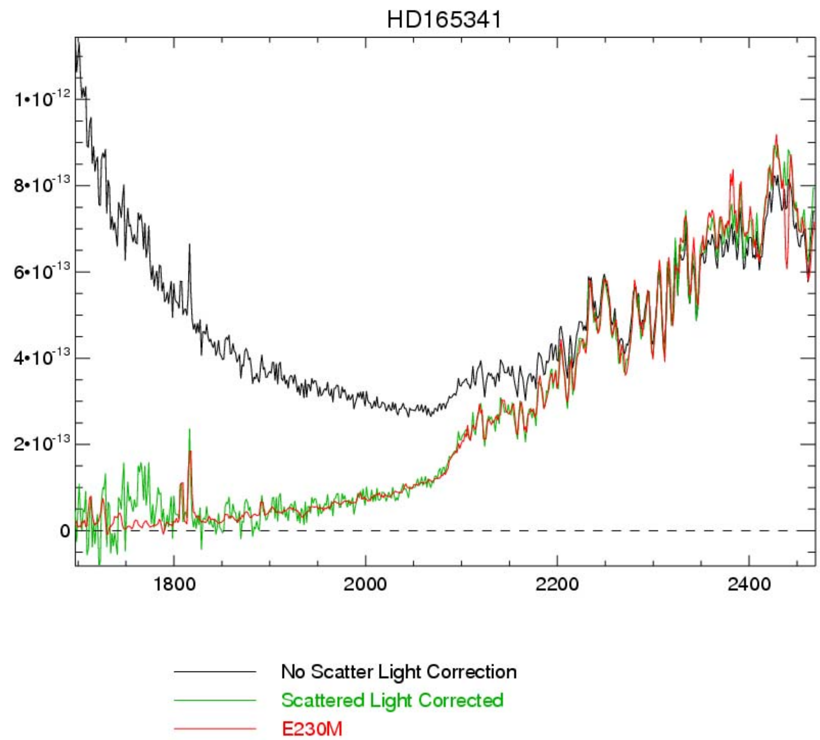

Figure 6: G230M scatter light correction compared to an E230M spectrum

3.2 Correction for position of the target within the Slit.

Significant photometric errors occur when the target star is not properly centered in the narrow 52X0.2 slit (as indicated in Figure 1). Fortunately, we can measure the offset of the targets from the center of the slit using the G750L fringe flats taken with the observation. If a target is centered in the slit, the fringes in the flat field observation will align with the fringes in the stellar observation. If the target is not centered, the offset between the fringes in the flat and the stellar spectra give you the offset within the slit.

Our first adjustment is for the change in the visual magnitude measured from the spectrum. Figure 7 shows the difference in the VT magnitude computed from the NGSL spectra and those tabulated in the Tycho II catalog plotted versus target offset from the center of the slit. A least square quadratic is fit to the difference (solid line in Figure 7) allows us to compute a scale factor to correct the observed spectral flux.

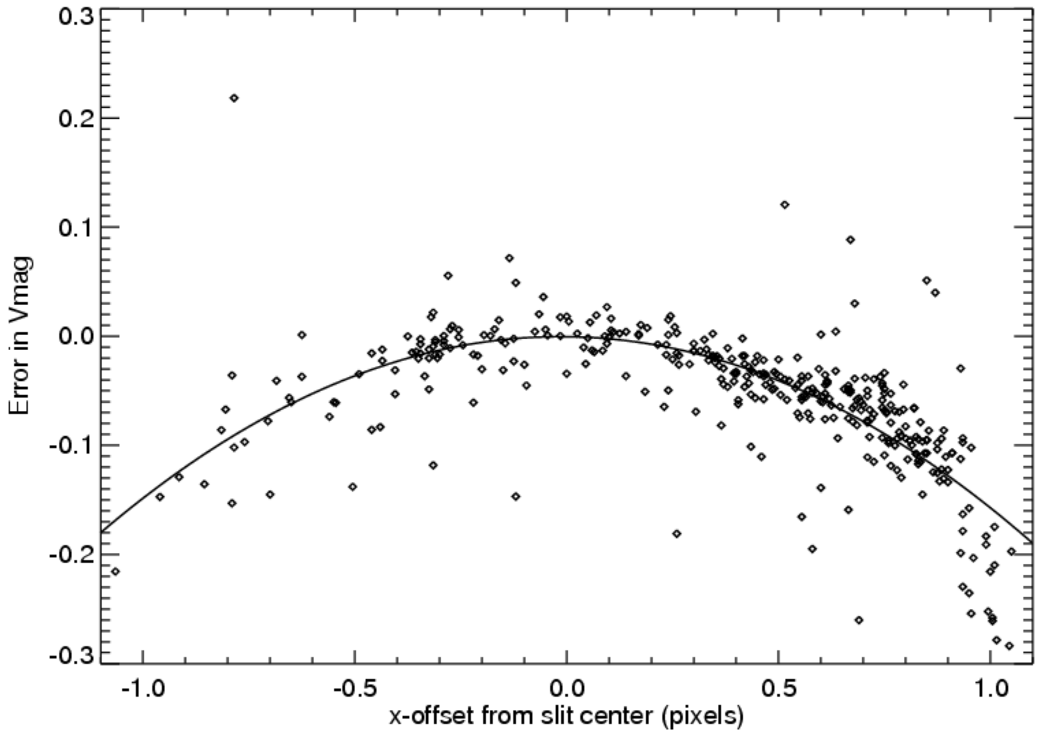

Figure 7: NGSL magnitude errors resulting when target is not centered within the slit.

Since the slit correction is wavelength dependent we investigated the B-V computed from the spectra as compared to the Tycho II values. Figure 8 shows the small systematic differences as a function of the target's position within the slit. We fit the residuals with a least squares cubic spline curve (solid curve in Figure 8) and used the fit to correct the spectra. The spectral flux is corrected with a correction factor (a linear function versus wavelength between 2900 and 5700 Angstroms normalized to 1.0 at 5300 Angstroms.). The slope of the function is computed to adjust the B-V to the center of the slit using the solid correction curve in Figure 8. The correction factor at 5700 Angstroms was used to correct all data above 5700 Angstroms. The 2900 Angstrom correction factor was used for all data below 2900 Angstroms.

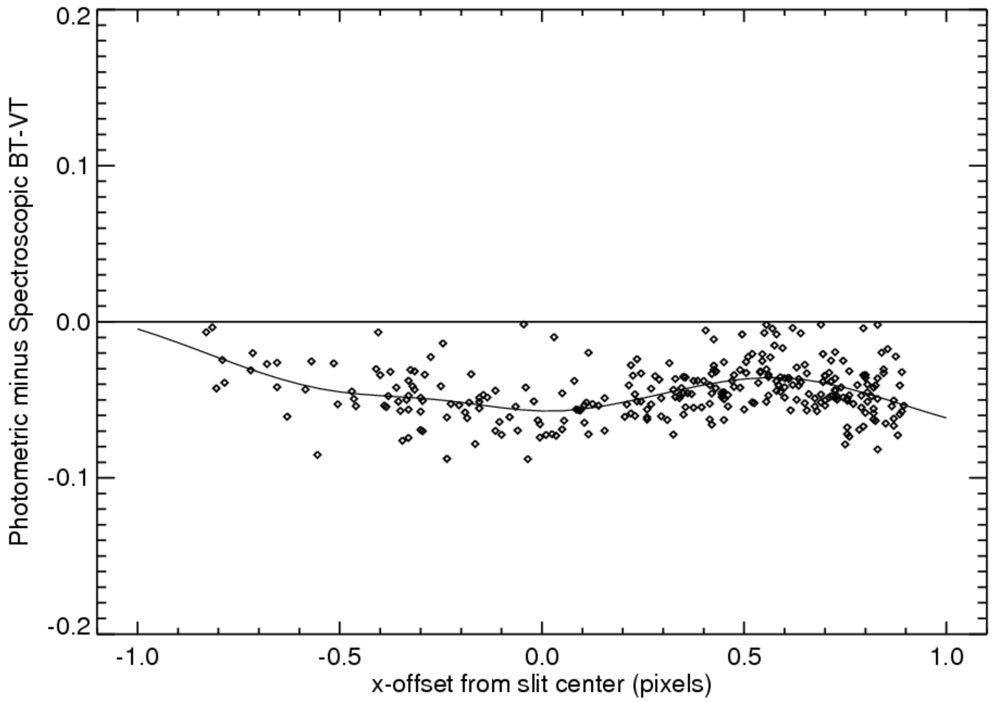

Figure 8: NGSL Spectroscopic BT-VT compared to Tycho II catalog values.

To correct wavelengths above 5700, we used best fit stellar models (using only the data below 5700 to determine the model parameters). We compared the ratio of the calibrated NGSL spectra to the model for wavelengths above 5700 Angstroms. Figure 9 shows the median ratio of the NGSL/Model spectra for various ranges of slit offsets. Figure 10 shows the flux ratios versus aperture position for all observations (plotted as diamonds) at various wavelengths (in 400 Angstrom bins). We fit a smooth spline curve versus slit offset to determine a correction for each wavelength bin. These corrections were then applied to the calibrated spectrum. Figure 11 shows the same plot as Figure 10 after the data has been corrected

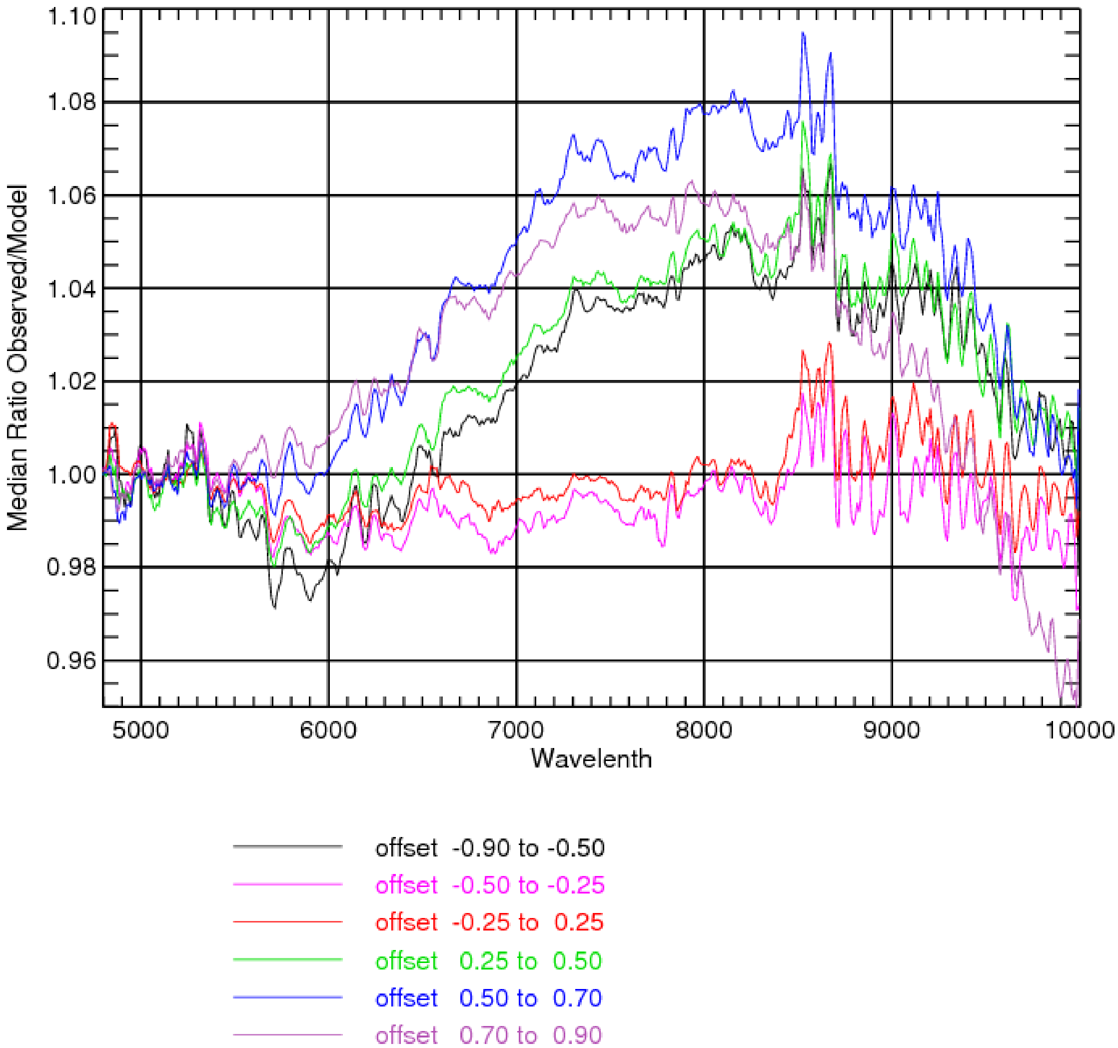

Figure 9: Flux errors when target is not centered within the target aperture.

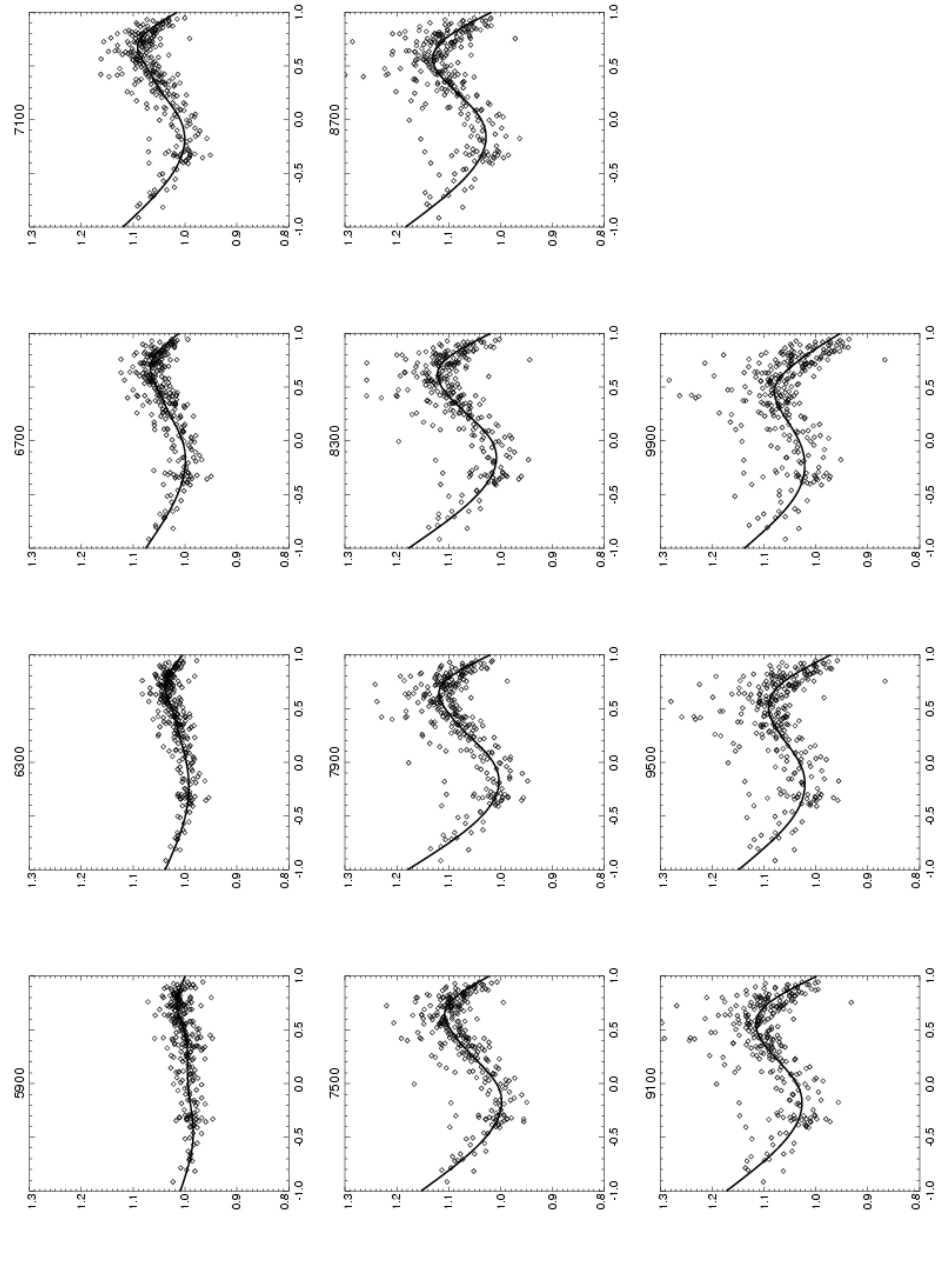

Figure 10: Flux correction versus position within the aperture in 400 Angstrom wavelength bins

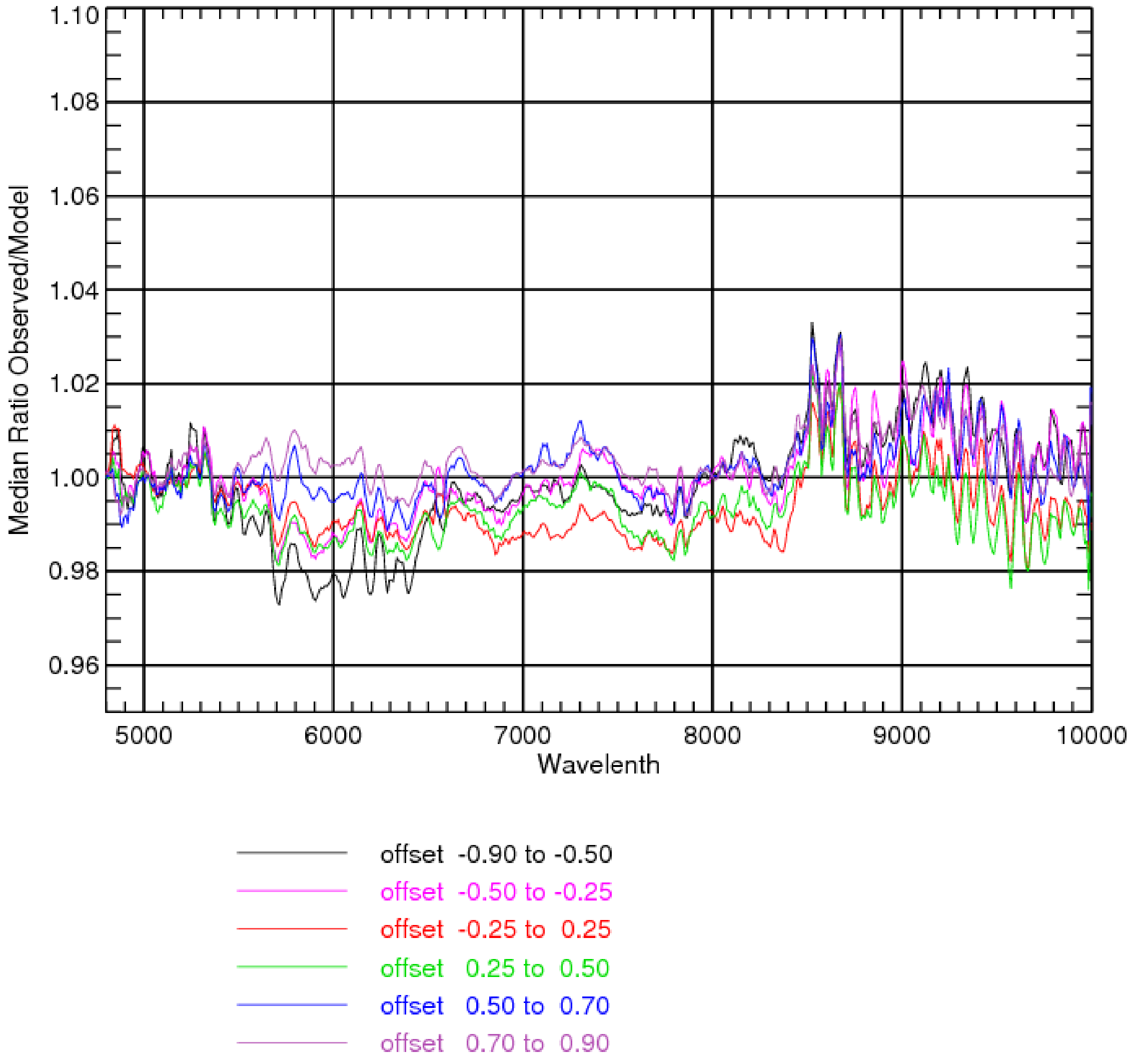

Figure 11: Observed NGSL spectra compared to the Munari models after correction for the offset of the target within the aperture.

As a final check of the slit correction we compared the ratio of the NGSL spectra with the matching spectra in the Miles ground base spectral library. Figure 12 shows the ratio (in 50 Angstrom bins) for various aperture offsets before correcting the NGSL spectra for the position of the star within the slit. Figure 13 shows the same comparison after slit correction. Results indicate that the slit correction is good to within a couple of percent and the overall sensitivity calibration of the Miles observations agree with the NGSL calibration to within approximately 3 percent from 3600 to 7300 Angstroms.

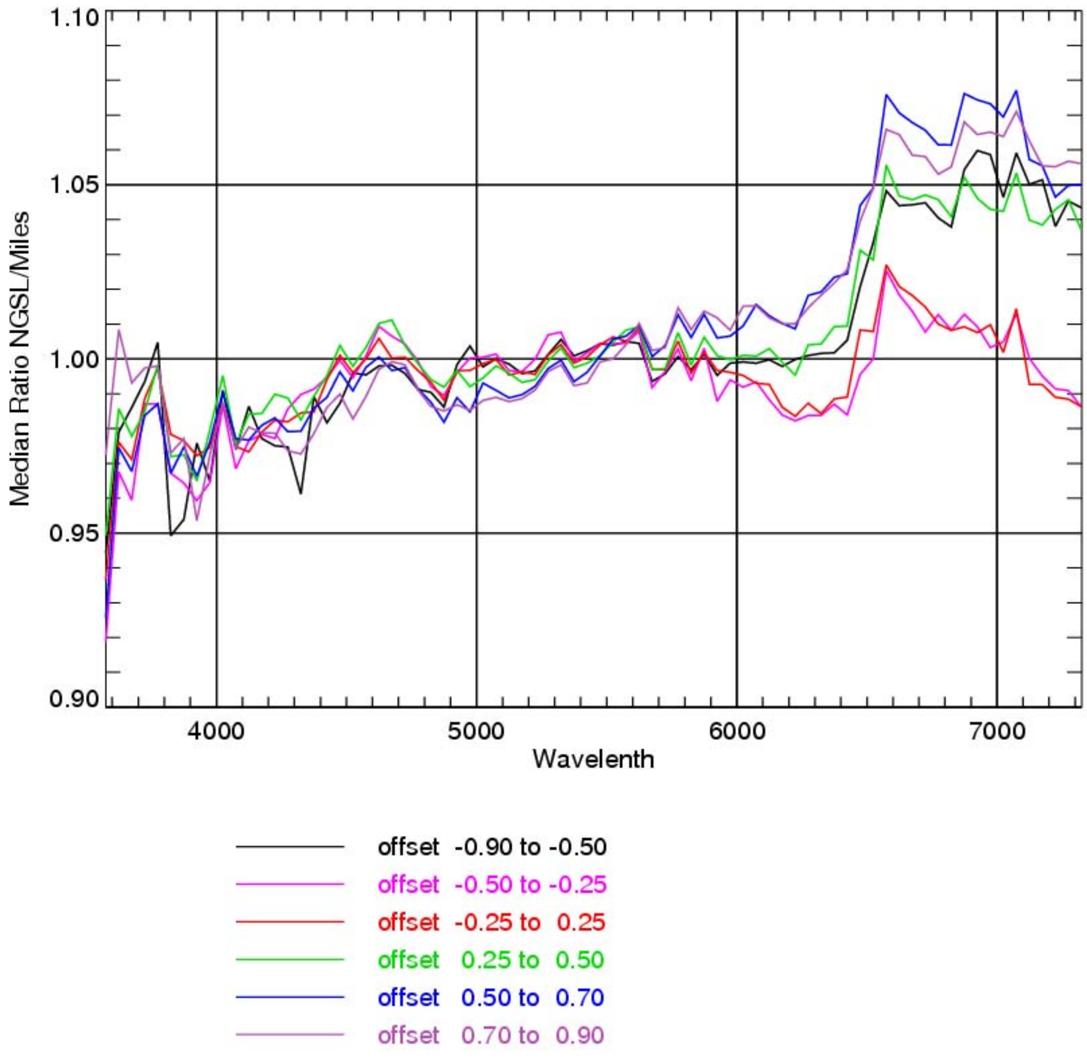

Figure 12: Comparison of the STIS NGSL spectra (without a slit correction) with the ground based Miles spectra for various offsets from the center of the slit.

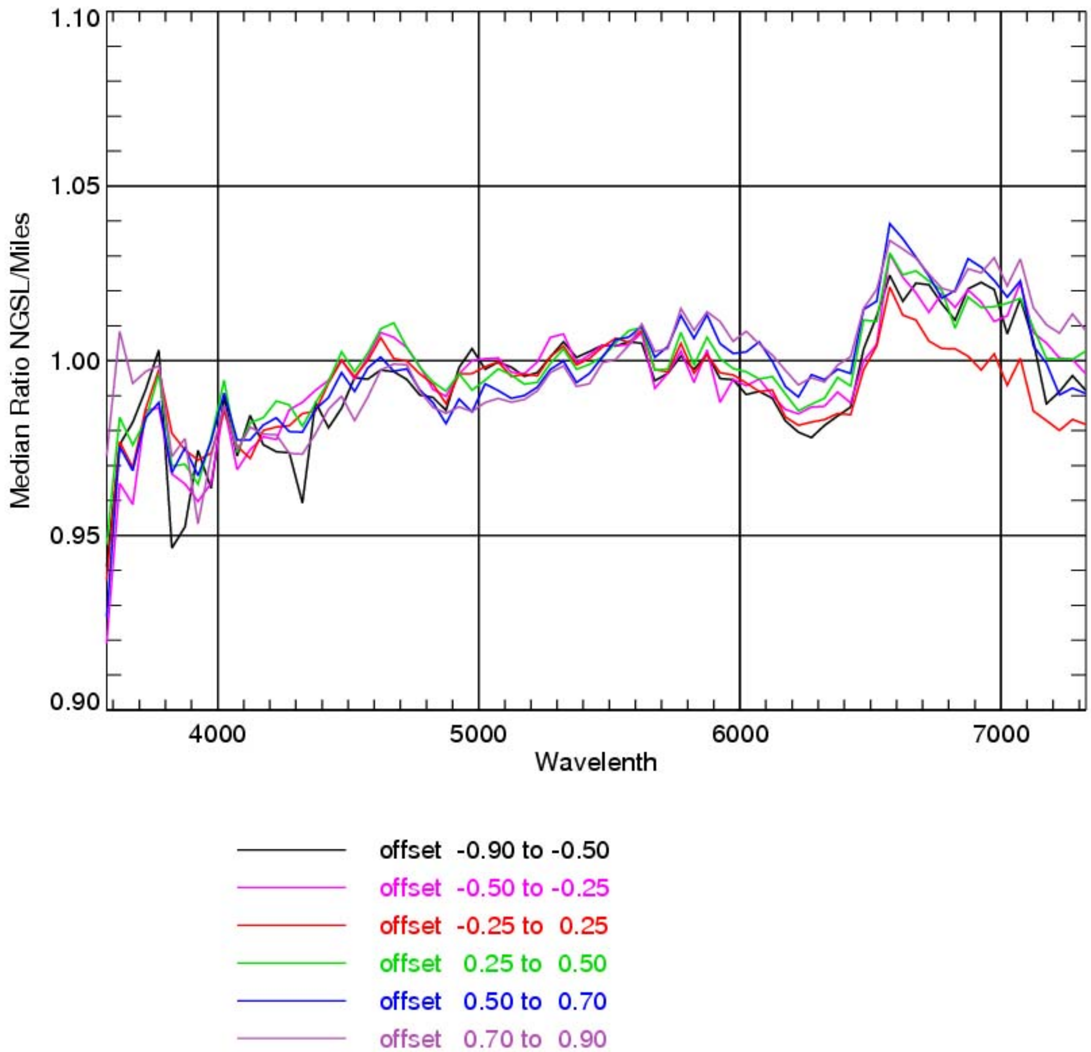

Figure 13: Comparison of the STIS NGSL spectra (after the slit correction) with the ground based Miles spectra for various offsets from the center of the slit.

4.0 Stellar Model Fitting

We estimated the effective temperature, surface gravity, metallicity, and reddening of NGSL stars by comparing the observed spectrum to spectral models by Castelli (2004). The least-squares fit attempts to minimize the RMS difference between the model and observed spectrum (both normalized to an average of 1.0 in the range of 4500 to 7000 Angstroms). The models were restricted to those falling on an Victoria-Regina isochrone (Vandenberg et al. 2006) The isochrone surface gravity was derived on the assumption that the target distance is within a two-sigma error of the distance in the new Hipparcos catalog. The following table gives the result for the best models. The fit quality (FITQUAL keyword in the header) is set to 1(good) if the RMS is less than 0.035. The quality is set to 2 (poor) if the RMS is between 0.035 and 0.08. If the RMS is above 0.08 or if no valid model good be found for the target (with the distance range from Hipparcos), no fit parameters are given.

Target Name	Data Quality	Fit Quality	FIT RMS	Teff	Log(g)	Log(Z)	alpha
BD+112998	good	1	0.022	5876.	2.8	-0.6	n
BD+363168	suspect	3					
BD+413306	good	1	0.027	5156.	4.5	-0.3	n
BD-122669	good	1	0.018	6960.	4.1	-1.9	a
BD092860	suspect	1	0.030	5926.	3.5	-0.7	a
BD174708	good	1	0.018	6174.	3.8	-1.9	a
BD292091	suspect	1	0.017	5803.	4.6	-2.0	a
BD371458	suspect	1	0.015	5463.	3.1	-2.0	a
BD413931	suspect	1	0.019	5486.	4.7	-1.8	a
BD423607	suspect	1	0.022	5963.	4.5	-2.0	a
BD442051	good	2	0.072	3741.	4.9	-0.3	n
BD511696	good	1	0.020	5776.	4.5	-1.3	a
BD592723	good	1	0.020	6419.	4.4	-2.0	a
BD660268	suspect	1	0.030	5453.	4.7	-1.8	a
BD720094	good	1	0.016	6286.	3.9	-2.0	a
CD-259286	suspect	1	0.018	6426.	3.0	-1.2	a
CD-3018140	suspect	1	0.015	6334.	3.9	-2.0	a
CD-621346	good	1	0.023	5652.	3.2	-0.6	n
CD-691618	good	3					
G019-013	good	1	0.027	4452.	4.6	-0.3	n
G021-024	suspect	2	0.037	4230.	4.7	-0.1	n
G029-023	good	1	0.019	6176.	3.7	-2.0	a
G114-26	good	1	0.019	6144.	4.1	-1.8	a
G115-58	suspect	1	0.023	6156.	3.7	-1.6	a
G12-21	suspect	1	0.020	6034.	4.1	-1.4	a
G13-35	good	1	0.016	6164.	3.9	-1.8	a
G169-28	suspect	1	0.019	5749.	3.9	-1.5	a
G17-25	suspect	1	0.022	5289.	4.6	-1.0	a
G18-39	good	1	0.017	5952.	3.6	-1.7	a
G18-54	good	1	0.022	5920.	3.8	-1.7	a

G180-24	good	1	0.018	6109.	4.0	-1.5	a
G187-40	suspect	1	0.017	5776.	4.0	-1.6	a
G188-22	suspect	1	0.016	5926.	3.9	-1.5	a
G188-30	suspect	1	0.030	5497.	4.6	-1.2	a
G192-43	suspect	1	0.017	6163.	3.9	-1.6	a
G194-22	suspect	1	0.018	6193.	4.1	-1.6	a
G196-48	suspect	1	0.013	5704.	3.4	-1.9	a
G20-15	suspect	1	0.017	6089.	4.1	-1.8	a
G202-65	suspect	1	0.028	6989.	4.4	-1.0	a
G231-52	suspect	1	0.023	5426.	4.7	-2.0	a
G234-28	good	1	0.019	6097.	3.9	-1.6	a
G24-3	good	1	0.018	6053.	3.9	-1.8	a
G243-62	suspect	1	0.028	4693.	4.8	-1.7	a
G260-36	suspect	1	0.026	5057.	4.5	0.1	n
G262-14	suspect	1	0.025	5085.	3.8	-0.7	a
G63-26	suspect	1	0.024	6123.	3.9	-1.6	a
G88-27	good	1	0.018	6141.	3.7	-1.6	a
GJ825	good	2	0.054	4015.	4.7	0.1	n
GL109	suspect	3					
GL15B	good	2	0.079	3741.	4.9	-0.2	n
HD000319	good	1	0.021	8195.	3.9	-0.4	n
HD000886	good	3					
HD001461	good	1	0.026	5790.	4.3	0.3	n
HD002665	good	1	0.011	5082.	2.2	-2.0	a
HD002857	suspect	2	0.036	7708.	2.8	-0.6	n
HD003360	good	3					
HD003712	suspect	1	0.022	4603.	1.8	-0.3	n
HD004128	suspect	1	0.021	4815.	2.3	-0.2	n
HD004727	good	3					
HD004813	good	1	0.024	6252.	4.3	-0.1	n
HD005256	good	1	0.021	5176.	3.6	-0.6	a
HD005395	good	1	0.018	4808.	2.5	-0.5	n
HD005544	good	1	0.016	4474.	1.7	-0.5	n
HD005916	good	1	0.017	4926.	2.5	-0.6	n
HD006229	good	1	0.017	5489.	2.5	-0.6	n
HD006734	good	1	0.021	4904.	3.1	-0.6	a
HD006755	good	1	0.013	5064.	2.6	-2.0	a
HD008491	good	1	0.019	4688.	2.5	-0.1	n
HD008724	suspect	1	0.019	4552.	1.3	-2.0	a
HD008890	good	3					
HD009051	suspect	1	0.012	4842.	2.0	-1.8	a
HD010380	good	1	0.015	4063.	1.2	-0.5	n
HD010780	good	1	0.024	5357.	4.4	0.1	n
HD012533	suspect	1	0.020	4225.	1.3	-0.2	n
HD013520	suspect	1	0.018	3920.	0.8	-0.6	n
HD015089	suspect	2	0.039	8823.	4.2	0.5	n
HD016031	suspect	1	0.017	6299.	3.9	-1.8	a
HD017072	good	1	0.020	5709.	3.1	-0.6	a
HD017081	good	1	0.029	13057.	3.6	-0.5	n
HD017361	good	1	0.019	4603.	2.4	-0.1	n
HD017925	good	1	0.022	5208.	4.5	0.1	n
HD018078	good	2	0.037	7404.	2.9	0.5	n

HD018769	good	1	0.028	8382.	4.1	0.5	n
HD018907	suspect	1	0.025	5309.	3.7	-0.1	n
HD019019	good	1	0.023	6197.	4.4	0.0	n
HD019308	good	1	0.022	5842.	4.1	0.2	n
HD019445	good	1	0.018	6200.	4.3	-1.9	a
HD019656	suspect	1	0.017	4563.	2.1	-0.3	n
HD019787	good	1	0.020	4771.	2.6	-0.1	n
HD020039	good	1	0.019	5200.	3.5	-0.6	a
HD020630	good	1	0.026	5687.	4.4	0.0	n
HD021742	good	1	0.024	5342.	4.4	0.4	n
HD022049	good	1	0.021	5130.	4.5	0.0	n
HD022484	good	1	0.023	6141.	4.1	0.1	n
HD023439	good	1	0.021	5249.	4.5	-0.6	a
HD025329	good	1	0.028	4930.	4.7	-1.1	a
HD025893	good	1	0.023	5342.	4.4	0.1	n
HD025975	good	1	0.020	4942.	3.3	0.0	n
HD026297	good	1	0.012	4423.	1.0	-2.0	a
HD026630	good	2	0.056	4542.	1.1	-2.0	a
HD027295	good	2	0.058	11548.	4.2	-0.4	n
HD028946	good	1	0.024	5389.	4.4	-0.0	n
HD028978	suspect	1	0.023	8749.	3.5	0.1	n
HD029391	good	1	0.027	7522.	4.3	0.2	n
HD029574	good	1	0.025	4049.	0.6	-1.7	a
HD030614	good	3					
HD030834	good	1	0.017	4008.	0.9	-0.6	n
HD031219	suspect	1	0.023	6087.	3.9	0.3	n
HD031421	good	1	0.018	4434.	1.9	-0.5	n
HD033793	good	3					
HD034078	good	3					
HD034797	suspect	2	0.036	12884.	4.1	0.0	n
HD034816	good	3					
HD036702	good	1	0.014	4319.	0.8	-2.0	a
HD036960	suspect	3					
HD037202	good	3					
HD037216	suspect	1	0.023	5437.	4.4	-0.0	n
HD037763	good	1	0.020	4597.	2.9	0.2	n
HD037828	good	1	0.012	4359.	1.0	-1.6	a
HD038237	good	1	0.025	8100.	3.9	0.1	n
HD038510	good	1	0.019	5897.	4.0	-0.8	a
HD039587	good	1	0.026	6057.	4.4	0.1	n
HD039833	good	1	0.027	5926.	4.3	0.2	n
HD040573	good	1	0.018	10200.	4.2	-0.4	n
HD041357	good	1	0.025	7578.	3.5	0.2	n
HD041661	good	1	0.019	6360.	3.2	-0.1	n
HD041667	suspect	1	0.019	4623.	1.8	-1.0	a
HD043042	suspect	1	0.022	6542.	4.2	0.0	n
HD044007	good	1	0.014	4930.	2.3	-1.8	a
HD045282	good	1	0.015	5199.	2.8	-1.8	a
HD046703	good	2	0.046	6484.	2.5	-0.0	n
HD047839	suspect	3					
HD048279	good	3					
HD050420	good	1	0.022	7167.	2.8	-0.0	n

HD052973	suspect	3					
HD055057	good	1	0.022	7289.	3.5	0.2	n
HD055496	suspect	1	0.024	4978.	2.1	-0.6	n
HD057060	suspect	3					
HD057061	suspect	3					
HD057727	good	1	0.020	4942.	2.9	-0.3	n
HD058343	suspect	3					
HD058551	good	1	0.020	6311.	4.2	-0.4	n
HD059612	good	3					
HD060319	good	1	0.018	5926.	4.0	-0.9	a
HD061064	good	1	0.021	6600.	3.4	0.2	n
HD061603	good	1	0.027	3841.	0.8	-0.3	n
HD062412	good	1	0.021	4876.	2.6	-0.1	n
HD063077	good	1	0.021	5926.	4.2	-0.7	a
HD063700	good	1	0.027	4498.	1.5	-0.5	n
HD063791	good	1	0.011	4778.	1.6	-2.0	a
HD064412	good	1	0.020	5742.	4.1	-0.6	a
HD065228	suspect	1	0.021	5926.	2.4	0.4	n
HD065354	good	1	0.021	3897.	0.8	-0.6	n
HD065714	good	1	0.023	4882.	2.2	0.0	n
HD067390	suspect	1	0.022	7193.	3.6	-0.2	n
HD068988	good	1	0.026	5897.	4.3	0.3	n
HD071160	good	1	0.017	3949.	0.9	-0.5	n
HD072184	good	1	0.019	4620.	2.6	0.1	n
HD072324	good	1	0.020	4793.	2.3	-0.1	n
HD072505	good	1	0.019	4519.	2.3	0.1	n
HD072968	suspect	2	0.066	9253.	3.9	0.5	n
HD073710	good	1	0.021	4897.	2.2	0.1	n
HD074088	good	1	0.028	3740.	0.5	-1.1	a
HD074721	good	1	0.027	8774.	3.3	-0.6	n
HD076291	good	1	0.017	4534.	2.3	-0.2	n
HD076932	good	1	0.019	6034.	4.1	-0.7	a
HD078316	good	2	0.073	12442.	3.7	-0.1	n
HD078362	good	1	0.028	7120.	3.8	0.5	n
HD078479	good	1	0.018	4476.	2.1	0.1	n
HD079158	good	3					
HD079349	suspect	1	0.027	3834.	1.1	-0.1	n
HD079469	good	1	0.027	10489.	4.2	-0.2	n
HD080607	good	1	0.023	5511.	3.7	0.4	n
HD081797	suspect	1	0.018	4188.	1.4	-0.1	n
HD082395	good	1	0.018	4664.	2.4	-0.3	n
HD082734	good	1	0.022	4949.	2.4	0.2	n
HD083212	good	1	0.014	4448.	1.2	-1.8	a
HD085380	good	1	0.024	6142.	4.0	0.2	n
HD086322	good	1	0.019	4687.	2.3	-0.3	n
HD086986	good	1	0.029	8230.	3.5	-1.2	a
HD087140	good	1	0.011	5093.	2.3	-2.0	a
HD087737	good	3					
HD090862	good	1	0.017	3937.	0.9	-0.6	n
HD091316	good	3					
HD093329	good	1	0.021	8323.	3.3	-0.6	n
HD093813	good	1	0.015	4264.	1.6	-0.5	n

HD094028	good	1	0.017	6104.	4.2	-1.4	a
HD095241	good	1	0.021	6034.	3.7	-0.1	n
HD095735	good	3					
HD095849	good	1	0.018	4459.	1.9	-0.0	n
HD096446	good	3					
HD097633	good	1	0.020	9107.	3.6	-0.2	n
HD099648	good	1	0.019	4811.	2.0	-0.3	n
HD101013	good	1	0.023	4837.	2.5	-0.0	n
HD101107	good	1	0.022	6937.	3.9	-0.1	n
HD102212	good	2	0.042	3800.	1.1	0.1	n
HD102780	good	1	0.032	3669.	0.5	-0.6	n
HD103036	suspect	1	0.013	4282.	0.8	-1.9	a
HD105452	good	1	0.023	7120.	4.2	-0.2	n
HD105546	good	1	0.016	5123.	2.3	-1.8	a
HD105740	good	1	0.016	4642.	2.2	-0.7	a
HD106304	suspect	1	0.015	9376.	3.6	-1.8	a
HD106516	good	1	0.020	6310.	4.3	-0.7	a
HD107582	good	1	0.022	5642.	4.3	-0.6	a
HD108945	suspect	1	0.033	8642.	3.9	0.5	n
HD109387	good	3					
HD109995	good	1	0.015	8251.	3.3	-1.6	a
HD110073	good	2	0.069	12041.	3.8	-0.4	n
HD110885	good	1	0.017	5823.	2.9	-0.8	a
HD111464	good	1	0.017	4004.	1.0	-0.6	n
HD111515	good	1	0.025	5549.	4.4	-0.3	n
HD111721	good	1	0.013	4911.	2.2	-1.9	a
HD111786	good	1	0.022	7598.	3.9	-1.3	a
HD112413	good	2	0.051	11687.	4.0	0.5	n
HD113002	good	1	0.020	5342.	2.7	-0.6	n
HD113092	good	1	0.015	4203.	1.3	-0.6	n
HD114330	suspect	1	0.021	9289.	3.6	-0.1	n
HD114710	good	1	0.026	6142.	4.4	0.2	n
HD115617	good	1	0.026	5557.	4.3	0.0	n
HD117880	suspect	1	0.029	9426.	3.7	-0.6	n
HD118055	good	1	0.014	4320.	0.9	-1.8	a
HD119971	good	1	0.019	4034.	1.1	-0.8	a
HD121146	good	1	0.017	4387.	2.2	-0.1	n
HD122064	good	1	0.021	4908.	4.5	0.4	n
HD122956	good	1	0.011	4625.	1.4	-2.0	a
HD123657	good	3					
HD124186	good	1	0.019	4420.	2.2	0.2	n
HD124425	good	1	0.020	6389.	3.6	-0.0	n
HD124547	suspect	1	0.016	4084.	1.2	-0.4	n
HD126327	suspect	3					
HD126511	good	1	0.025	5486.	4.3	0.2	n
HD126614	good	1	0.027	5437.	4.0	0.5	n
HD126661	good	1	0.028	7757.	3.6	0.4	n
HD128000	good	1	0.025	3837.	0.9	-0.4	n
HD128279	good	1	0.013	5456.	3.0	-2.0	a
HD128801	good	1	0.014	10123.	3.7	-1.9	a
HD128987	suspect	1	0.025	5537.	4.4	-0.0	n
HD131873	good	1	0.017	3926.	0.9	-0.6	n

HD132345	good	1	0.023	4442.	2.3	0.2	n
HD132475	good	1	0.016	5687.	3.6	-1.6	a
HD134113	good	1	0.022	5820.	3.9	-0.6	a
HD134439	suspect	1	0.032	5130.	4.7	-1.5	a
HD134440	good	1	0.028	4970.	4.7	-1.1	a
HD136726	good	1	0.016	4093.	1.3	-0.4	n
HD137759	suspect	1	0.028	4563.	2.3	-0.2	n
HD137909	suspect	2	0.045	7663.	3.8	0.0	n
HD138716	suspect	1	0.019	4771.	2.9	-0.1	n
HD138749	suspect	2	0.066	14141.	3.8	-0.6	n
HD140232	good	1	0.028	8157.	4.2	0.5	n
HD141795	good	1	0.026	8419.	4.2	0.3	n
HD141851	good	1	0.021	8231.	4.0	-0.2	n
HD142091	good	1	0.020	4749.	2.9	-0.1	n
HD142703	good	1	0.017	7337.	3.9	-1.4	a
HD142860	suspect	1	0.023	6397.	4.2	-0.1	n
HD142926	good	1	0.035	11908.	3.8	0.1	n
HD143107	suspect	1	0.015	4303.	1.7	-0.4	n
HD143459	good	1	0.023	9878.	3.6	-0.6	n
HD145328	suspect	1	0.020	4764.	2.8	-0.2	n
HD146051	good	2	0.040	3667.	0.7	-0.3	n
HD146233	suspect	1	0.024	5842.	4.4	0.1	n
HD147394	good	3					
HD147550	good	1	0.033	10074.	3.9	-0.0	n
HD148293	good	1	0.021	4642.	2.4	0.0	n
HD148513	good	1	0.021	4003.	1.3	-0.3	n
HD149161	good	1	0.022	3884.	1.1	-0.3	n
HD149382	good	3					
HD155763	good	3					
HD156283	good	1	0.018	4133.	1.3	-0.1	n
HD157244	good	1	0.027	4206.	1.3	-0.1	n
HD159181	good	2	0.080	4542.	1.5	-0.6	n
HD160346	good	1	0.023	5004.	4.5	0.1	n
HD160762	good	3					
HD160922	good	1	0.023	6600.	4.0	0.0	n
HD161770	good	1	0.017	5818.	3.8	-1.6	a
HD163346	good	2	0.074	5597.	2.5	-0.6	n
HD163641	good	2	0.041	11482.	3.9	-0.1	n
HD163810	suspect	1	0.019	5876.	4.4	-1.2	a
HD164058	good	1	0.024	3896.	0.9	-0.4	n
HD164257	good	2	0.043	7977.	3.5	-0.1	n
HD164353	good	3					
HD164402	good	3					
HD164967	good	1	0.026	8534.	4.1	-0.6	n
HD165195	good	1	0.034	4060.	0.6	-1.8	a
HD165341	good	1	0.022	5319.	4.4	0.1	n
HD166208	good	1	0.025	5107.	2.3	0.0	n
HD166229	good	1	0.020	4576.	2.5	0.1	n
HD166283	good	1	0.028	8289.	4.1	0.1	n
HD166991	good	1	0.021	8497.	4.0	-0.3	n
HD167006	good	2	0.059	3536.	0.4	-0.3	n
HD167105	suspect	1	0.031	8574.	3.4	-0.6	n

HD167278	suspect	1	0.023	6609.	4.2	-0.1	n
HD167946	good	1	0.030	10634.	4.3	-0.1	n
HD169191	good	1	0.015	4245.	1.6	-0.4	n
HD170737	good	1	0.017	4942.	3.0	-0.9	a
HD170756	good	2	0.040	6252.	2.4	-0.0	n
HD170973	good	2	0.064	10676.	3.3	0.5	n
HD172230	good	1	0.030	7542.	3.4	0.5	n
HD172506	suspect	1	0.027	7226.	4.1	0.0	n
HD173158	good	2	0.038	3856.	0.5	-1.3	a
HD173819	suspect	2	0.071	3714.	0.6	-0.6	a
HD174240	good	1	0.019	9274.	3.8	-0.2	n
HD174959	suspect	1	0.030	14123.	3.7	-0.6	n
HD174966	suspect	1	0.025	7693.	4.0	0.1	n
HD175156	good	3					
HD175305	suspect	1	0.016	5037.	2.5	-1.6	a
HD175545	good	1	0.018	4420.	2.4	0.0	n
HD175640	good	2	0.057	11237.	3.9	-0.2	n
HD175674	good	1	0.022	4242.	1.6	-0.1	n
HD175805	good	1	0.021	6274.	3.6	0.2	n
HD175865	suspect	3					
HD176232	suspect	1	0.030	7615.	3.9	0.3	n
HD176437	good	3					
HD181720	good	1	0.021	5709.	3.9	-0.6	a
HD183324	suspect	1	0.024	8673.	4.1	-1.1	a
HD183915	good	1	0.022	4319.	1.4	-0.4	n
HD184266	suspect	1	0.018	6109.	3.0	-1.1	a
HD185144	good	1	0.022	5293.	4.5	-0.1	n
HD185351	good	1	0.020	4904.	3.0	-0.1	n
HD187111	good	1	0.015	4423.	1.1	-1.8	a
HD187879	good	3					
HD188262	suspect	3					
HD190073	good	3					
HD190360	good	1	0.027	5531.	4.2	0.2	n
HD190404	good	1	0.026	5110.	4.6	-0.3	n
HD191026	good	1	0.022	5149.	3.7	0.1	n
HD191277	good	1	0.018	4476.	2.5	0.1	n
HD193281	good	1	0.018	8249.	3.6	-0.6	n
HD193495	good	3					
HD194093	suspect	3					
HD194453	suspect	1	0.023	10241.	3.9	0.0	n
HD195434	suspect	1	0.026	5152.	4.6	-0.5	n
HD196218	good	1	0.023	6367.	4.2	0.0	n
HD196426	good	1	0.029	12800.	4.0	-0.5	n
HD196662	suspect	1	0.031	14204.	3.7	-0.6	n
HD196725	good	1	0.022	4003.	0.9	-0.6	n
HD196892	good	1	0.018	6086.	4.1	-1.0	a
HD197177	good	1	0.019	4748.	1.9	-0.4	n
HD198809	good	1	0.020	5291.	2.9	-0.0	n
HD200081	good	1	0.034	5120.	2.6	-0.5	n
HD200905	good	1	0.030	3793.	0.6	-0.6	n
HD201091	good	1	0.030	4404.	4.6	-0.1	n
HD201377	good	1	0.023	8084.	3.9	0.0	n

HD201601	good	1	0.034	7631.	4.0	-0.1	n
HD203638	good	1	0.020	4520.	2.3	-0.1	n
HD204041	good	1	0.020	8260.	4.2	-0.6	n
HD204155	good	1	0.019	5787.	3.9	-0.6	a
HD204543	suspect	1	0.014	4667.	1.4	-2.0	a
HD204867	suspect	3					
HD205202	good	1	0.019	6564.	3.6	-0.6	a
HD205811	good	1	0.021	9287.	4.2	-0.1	n
HD206778	good	1	0.030	4095.	1.3	0.1	n
HD210745	good	1	0.033	4003.	0.9	-0.6	n
HD210807	good	1	0.018	4926.	2.3	-0.3	n
HD212516	good	2	0.044	3578.	0.5	-0.5	n
HD212593	good	3					
HD215665	good	1	0.019	4752.	2.0	-0.2	n
HD217107	good	1	0.027	5631.	4.2	0.4	n
HD217357	good	2	0.042	4153.	4.7	-0.3	n
HD221377	good	1	0.020	6556.	3.9	-0.6	n
HD222404	good	1	0.022	4790.	3.1	0.1	n
HD224801	good	2	0.062	11757.	3.9	0.5	n
HD224926	good	2	0.042	13499.	3.8	-0.5	n
HD232078	suspect	2	0.072	3640.	0.5	-0.6	n
HD284248	suspect	1	0.016	6171.	4.0	-1.8	a
HD345957	good	1	0.017	5920.	3.8	-1.4	a
HR0753	suspect	1	0.030	4882.	4.7	-0.2	n
HR8086	suspect	2	0.047	4230.	4.7	-0.7	a
VBNVUL	suspect	2	0.046	6937.	2.4	-0.5	n
VGKCOM	suspect	3					
VIWCOM	good	3					